A High Accuracy FDTD Algorithm to Solve Microwave Propagation and Scattering Problems on a Coarse Grid

James B. Cole

Abstract—**If the spatial variation of electric permittivity and magnetic permeability is "small" Maxwell's equations can be approximated by the scalar wave equation in each field component. We introduce a new high-accuracy second order finite-difference time-domain (FDTD) algorithm to solve the scalar wave equation on a coarse grid with a solution error less than 10^{-4} that of the conventional one. The computational load at each grid point is greater, but it is more than offset by a large reduction in the number of grid points needed, as well as by a reduction in the number of iterations. Also boundaries can be more accurately characterized at the subgrid level. Although optimum performance is achieved at a fixed frequency, the accuracy is still much higher than that of a conventional FDTD algorithm over "moderate" bandwidths.**

I. Introduction

MANY ELECTROMAGNETIC problems can be reduced to the scalar wave equation in each field component if the spatial variation of electric permittivity and magnetic permeability is "sufficiently small." In many practical problems magnetic permeability can be regarded as constant, with constant electrical permittivity except at certain interfaces. For example, for TM waves ($E_x = E_y = 0$, $E_z \neq 0$; $H_z = 0$, $H_x \neq 0$, $H_y \neq 0$) incident on some conducting structure in vacuum, Maxwell's equations reduce to the scalar wave equation with respect to E_z.

We introduce a new high accuracy finite-difference time-domain (FDTD) algorithm to solve the scalar wave equation with sources and attenuation. We have coupled this algorithm with (computational) real time visualizations that allow the user to view wave propagation and scattering processes as the computation proceeds. The algorithm is thus a useful tool for modeling transient phenomena. In addition since the far field approximation is not used, this algorithm is useful to compute near field processes.

The homogeneous wave equation

$$(\partial_{tt} - v(x)^2\nabla^2)\psi(x,t) = 0 \tag{1}$$

where $v(x) = \frac{1}{\sqrt{\varepsilon(x)\mu(x)}}$ is the local wave speed, can be approximated by a finite-difference (FD) equation of the form [1]

$$(\mathbf{T} - v(x)^2\mathbf{D})\psi(x,t) = 0 \tag{2}$$

where $\mathbf{T}$ and $\mathbf{D}$ are FD approximations to ∂_{tt} and ∇^2, respectively. Solution error arises from the deviation of $\mathbf{T}\psi$ and $\mathbf{D}\psi$ from $\partial_{tt}\psi$ and $\nabla^2\psi$. It can be reduced either by using higher order FD approximations, or by finer space-time sampling of the wavefield. Unfortunately both strategies are computationally expensive, and the tradeoff between accuracy and computational economy is quite severe. It is thus desirable to improve the accuracy without going to higher order approximations, and without increasing the fineness of the computational grid. That is the subject of this paper.

FD solutions to (1) are plagued not only by the absolute size of the solution error but also by its anisotropy with respect to the propagation direction due to the anisotropy of the FD Laplacian. In this paper we introduce a new, nearly isotropic, second-order FD Laplacian, which when inserted into a modified version of (2), yields a second-order FDTD wave propagation algorithm that is almost error free on a coarse grid at fixed wave number and frequency. Even over a "moderate" frequency band, however, the error is still smaller than that of a conventional FDTD algorithm. Our isotropic FD Laplacian can also be used in other types of FD equations to improve the accuracy.

II. A Nearly Isotropic Second-Order Finite-Difference Laplacian

For simplicity, let us first restrict ourselves to two dimensions. On a uniform Cartesian grid, there are two possible second-order FD approximations to the Laplacian defined by

$$h^2\mathbf{D}_1 f(x,y) = f(x+h,y) + f(x-h,y) + f(x,y+h) + f(x,y-h) - 4f(x,y) \tag{3a}$$

and

$$h^2\mathbf{D}_2 f(x,y) = \frac{1}{2}[f(x+h,y+h) + f(x+h,y-h) + f(x-h,y+h) + f(x-h,y-h)] - 2f(x,y) \tag{3b}$$

where h is the grid spacing. A general second-order FD Laplacian can thus be expressed as a linear combination of $\mathbf{D}_1$ and $\mathbf{D}_2$ in the form

$$\mathbf{D} = \gamma\mathbf{D}_1 + (1-\gamma)\mathbf{D}_2 \tag{4}$$

where γ is a real parameter.

Manuscript received August 3, 1994; revised May 25, 1995. This work was supported by the Office of Naval Research and the Naval Research Laboratory.

The author is with the Naval Research Laboratory, Washington, DC, USA. He is currently on leave at Tsukuba University, Department of Information Sciences and Electronics, Tsukuba 305, Japan.

IEEE Log Number 9413429.

The spatial part of a plane wave solution to (1) is $\psi_s(x) = e^{\imath k \bullet x}$, where $k = (k_x, k_y) = k(\cos\theta, \sin\theta)$, $x = (x, y)$, and $k = 2\pi/\lambda$, where λ is the wavelength. If λ is expressed in terms of the grid spacing, we can then set $h = 1$.

Throughout this paper we take $h = 1$, and λ/h is replaced by λ measured in grid units. The important quantity in a wave propagation and scattering problem is not the absolute wavelength but its size relative to the grid spacing and to the scattering features. Applying $\mathbf{D}$ to ψ_s with $h = 1$ we find that $\mathbf{D}\psi_s = 2\psi_s D$, where

$$D(k,\theta) = \gamma D_1(k,\theta) + (1-\gamma)D_2(k,\theta) \tag{5a}$$

and

$$D_1(k,\theta) = \cos k_x + \cos k_y - 2, \tag{5b}$$

$$D_2(k,\theta) = \cos k_x \cos k_y - 1. \tag{5c}$$

Although both D_1 and D_2 are anisotropic with respect to the propagation direction, θ, we might hope to find a value of γ that makes D isotropic.

Since $D_1(k,0) = D_2(k,0) = \cos k - 1$, let us try to determine γ such that $D(k,\theta) = \cos k - 1$. At one arbitrary value of θ this can be done by choosing

$$\gamma(k,\theta) = \frac{D_2(k,\theta) - (\cos k - 1)}{D_2(k,\theta) - D_1(k,\theta)}. \tag{6}$$

At first sight this approach does not look very promising, because the constant parameter that we seek is a function of both k and θ. It turns out, however, that the θ-dependence of γ is quite weak and we can eliminate it by evaluating γ at a fixed value of θ, θ_0.

Defining

$$D_0(k,\theta) = \gamma_0(k)D_1(k,\theta) + (1-\gamma_0(k))D_2(k,\theta) \tag{7}$$

where

$$\gamma_0(k) = \gamma(k,\theta_0). \tag{8}$$

Let us examine the anisotropy of D_0 [see Fig. 1(b)]. We find that the choice $\theta_0 = 0.18203\pi$ symmetrizes $\Delta D_0(k,\theta)/(\cos k - 1)$ about zero such that its maxima and minima have the same absolute values. This symmetrization is, moreover, independent of k to an excellent approximation. Comparing Fig. 1(a) and (b) we see that the anisotropy of D_0 is less than 10^{-4} that of D_1 on a coarse grid ($\lambda = 8$), and

$$D_0(k,\theta) \approx \cos k - 1 \tag{9}$$

is thus an excellent approximation for all θ. The linear combination

$$\mathbf{D}_0(k) = \gamma_0(k)\mathbf{D}_1 + (1-\gamma_0(k))\mathbf{D}_2 \tag{10}$$

thus constitutes a nearly isotropic finite difference Laplacian expression for ∇^2. While $\nabla^2 e^{ik\bullet r}/e^{\imath k\bullet x} = -k^2$, $\mathbf{D}_0 e^{ik\bullet x}/e^{ik\bullet x} \approx 2(\cos k - 1) = -k^2 + 2k^4/4! + \mathrm{L}$, so $\mathbf{D}_0$ is still fundamentally a second order approximation to ∇^2,

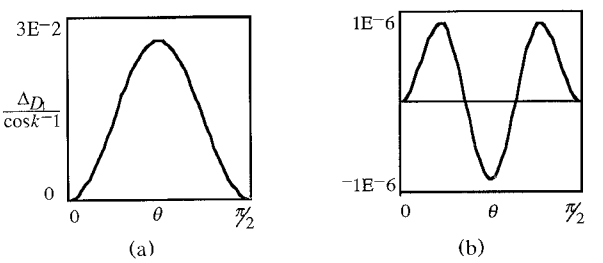

Fig. 1. Anisotropy of $\mathbf{D}_1$ and $\mathbf{D}_0$ at $k = 2\pi/8$. $\Delta D(k,\theta) = D(k,\theta) - (\cos k - 1)$, where $D = D_1$ or D_0.

but unlike $\mathbf{D}_1 e^{\imath k\bullet r}/e^{\imath k\bullet r}$ and $\mathbf{D}_2 e^{\imath k\bullet r}/e^{ik\bullet x}$, $\mathbf{D}_0 e^{ik\bullet x}/e^{\imath k\bullet x}$ is virtually isotropic.

Since γ_0 is a function of k, we would expect that this isotropy can be valid only at the wave number, k_0, used to compute γ_0. It turns out, however, that while the isotropy of $\mathbf{D}_0$ does degrade away from k_0, it is still much better than that of $\mathbf{D}_1$. This point is discussed further in Appendix A.

III. A Nearly Exact Second Order Algorithm

Let us take $\mathbf{T}$ to be the standard second-order FD operator given by

$$\tau^2 \mathbf{T} f(t) = f(t+\tau) + f(t-\tau) - 2f(t) \tag{11}$$

where τ is the time step size. Setting $\tau = 1$, and computing $\mathbf{T}e^{-\imath\omega t}$ we find $\mathbf{T}e^{-\imath\omega t} = 2T(\omega)e^{-\imath\omega t}$, where $T(\omega) = \cos\omega - 1$. Here $\omega = 2\pi/P$, where P is the wave period measured in terms of time steps. Throughout this paper we take $\tau = 1$, and P/τ is replaced by P measured in time steps.

The nearly exact isotropy of $\mathbf{D}_0$ allows us, at fixed wave number and frequency, to construct a nearly exact algorithm to solve (1) by modifying the form of (2). Since $\mathbf{D} = \mathbf{D}_0$ is nearly isotropic, the deviation of $\mathbf{T}$ and $\mathbf{D}$ from ∂_{tt} and ∇^2 can be compensated for by replacing v in (2) by an adjustable parameter, u

$$(\mathbf{T} - u^2\mathbf{D})\psi(x,t) = 0. \tag{12}$$

Setting $\mathbf{D} = \mathbf{D}_0$, and substituting a plane wave, $\psi_0(x,t) = e^{\imath(k\bullet x - \omega t)}$, into (12), we obtain

$$(\mathbf{T} - u^2\mathbf{D}_0)\psi_0(x,t) = 2\psi_0(x,t)\varepsilon(\omega,k,\theta) \tag{13}$$

where $\varepsilon(\omega,k,\theta) = T(\omega) - u^2 D_0(k,\theta)$ is the solution error. Using (9), ε can be made to vanish at fixed k and w, by choosing $u = u_0$, where

$$u_0^2 = \frac{\cos\omega - 1}{\cos k - 1}. \tag{14}$$

Insofar as (9) holds, the solution error vanishes at fixed k and ω. The choices $(\mathbf{D} = \mathbf{D}_0, u = u_0)$ in (12) thus define the optimal finite difference approximation to (1). The replacement of v by u is actually a generalized application of the methodology described in [6].

We can now construct an FDTD algorithm to solve the wave equation of the form

$$\psi(x,t+1) = 2\psi(x,t) - \psi(x,t-1) + u(x)^2 \mathbf{D}\psi(x,t). \tag{15a}$$

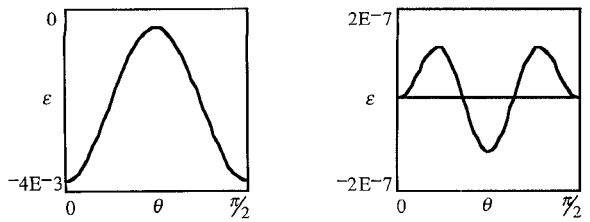

Fig. 2. Solution error anisotropy for (a) the $(\mathbf{D} = \mathbf{D}_1, u = v)$ and (b) the $(\mathbf{D} = \mathbf{D}_0, u = u_0)$ algorithms at $k = 2\pi/8$, and $\omega/k = 2/3$.

We write $u(x)$ to emphasize that u can vary spatially. For the inhomogeneous wave equation with sources and attenuation [2]

$$(\partial_{tt} - v(x)^2\nabla^2)\psi(x,t) = v(x)^2 s(x,t) - 2\alpha(x)\partial_t\psi(x,t) \quad (16)$$

where $s(x,t)$ is a source term and α is the attenuation, it can be shown [3] that (15a) becomes

$$\psi(x,t+1) = \psi(x,t) + \left(\frac{1-2\alpha(x)}{1+2\alpha(x)}\right)(\psi(x,t) - \psi(x,t-1)) + \left(\frac{1}{1+2\alpha(x)}\right)u(x)^2(\mathbf{D}\psi(x,t) + s(x,t)). \quad (15b)$$

If the refractive index of the medium depends on position, then at fixed frequency $k = k(x)$, and we can define $\mathbf{D}_0$ and u_0^2 locally as functions of position. In the case of locally variable permittivity, $\varepsilon(x)$, and conductivity, $\sigma(x)$, we can replace $(1-2\alpha)/(1+2\alpha)$, and $1/(1+2\alpha)$ by $(2\varepsilon-\sigma)/(2\varepsilon+\sigma)$, and $2/(2\varepsilon+\sigma)$, respectively (see for example Ref. 7). Boundaries can also be accommodated by a local definition of $\mathbf{D}$ as shown in Section VI.

Because we sample only points adjacent to x, on a single-instruction multiple-data (SIMD) computing architecture, interprocessor communication is minimized and this algorithm can be rapidly iterated. Using time-domain display graphics output we have viewed the evolution of wave propagation and scattering processes in complicated environments [3]–[5].

In Fig. 2 we compare the absolute size and anisotropy of solution error (ε) as a function of θ for the choices $(\mathbf{D} = \mathbf{D}_1, u = v)$ and $(\mathbf{D} = \mathbf{D}_0, u = u_0)$. We see that for the latter $|\varepsilon|$ is more than four orders of magnitude smaller than for the former.

The primary source of solution error at a single frequency is due to the error in the phase, rather than the amplitude, of the computed wavefronts. When (15a) is iterated, a mode of wave number k and frequency ω will appear to propagate with a velocity v' such that (12) is satisfied. Denoting by $\Delta v'$ the maximum amount by which v' deviates from $v = \omega/k$, the maximum distance, R, that a wave front can propagate on the grid before the phase error accumulates to $2\pi/\lambda$ is

$$R = \frac{v'}{\Delta v'}. \quad (17)$$

For example at $\lambda = 8$ and $\omega/k = 2/3$, $R/\lambda = 8.6$ for $(\mathbf{D} = \mathbf{D}_1, u = v)$, whereas for $(\mathbf{D} = \mathbf{D}_0, u = u_0)$ $R/\lambda = 2.8 \times 10^5$.

IV. Stability Conditions and Simulation Speed

Equation (12) can expressed in the form

$$\psi_{t+1} - 2\psi_t + \psi_{t-1} = 2u^2 D\psi_t \quad (18)$$

where, for simplicity, the spatial dependence is suppressed and discretized time is denoted by a subscript. Postulating a solution of the form $\psi_t = w^t$ and inserting it into (18), we obtain $w^2 - 2bw + 1 = 0$, where $b = 1 + u^2 D$. For (18) to have an oscillatory solution we must have $b^2 < 1$. This implies the constraint $u^2 < -D$. Following Ref. [1], the upper bound on u^2 is determined by the maximum possible value of $(-D)$, which yields

$$u^2 < \frac{2}{\max(-D)}. \quad (19)$$

The stability condition can be expressed in the form $\lambda/P = v < v_{\max}$, which can be rewritten as

$$P > \frac{\lambda}{v_{\max}} \quad (20)$$

where $v_{\max}$ is determined from (19). Since λ and P are measured in terms of grid units and time steps, respectively, the wave velocity, $v = \lambda/P$, represents the number of grid units that the wavefront propagates per time step. The larger $v_{\max}$, the fewer the number of iterations needed to solve a given problem.

For $(\mathbf{D} = \mathbf{D}_1, u = v)$, $\max(-D) = 4$ and (19) yields the well known constraint

$$v_{\max}(\mathbf{D} = \mathbf{D}_1, u = v) = \frac{\sqrt{2}}{2} \approx 0.70. \quad (21)$$

For $(\mathbf{D} = \mathbf{D}_0, u = u_0)$, $\max(-D) = 4\gamma_0$ and we find that $u_0^2 < 1/(2\gamma_0)$. Using the facts that $\lim_{k\to 0}\gamma_0(k) = 2/3$ and $\gamma_0(k > 0) < 2/3$, we obtain $u_0^2 < 3/4$ for all $k > 0$. Inserting $\omega = kv$ into (14), we obtain

$$v_{\max} = \frac{2}{k}\arcsin\left(\frac{\sqrt{3}}{2}\sin(k/2)\right). \quad (22)$$

What value of k should we use to evaluate $v_{\max}$? An arbitrary signal contains a mix of frequencies, so to ensure stability we must use the minimum value of $v_{\max}$ with respect to k. Since $v_{\max}$ decreases as k increases, we use $k_{\max} = 2\pi/3$, which corresponds to $\lambda = 3$, the shortest wavelength that can propagate on the grid (see Appendix B). Thus

$$v_{\max}(\mathbf{D} = \mathbf{D}_0, u = u_0) = \frac{3}{\pi}\arcsin\left(\frac{3}{4}\right) \approx 0.80 \quad (23)$$

which is about 14% larger than $v_{\max}(\mathbf{D} = \mathbf{D}_1, u = v)$.

The $(\mathbf{D} = \mathbf{D}_0, u = u_0)$ algorithm thus requires fewer iterations than the $(\mathbf{D} = \mathbf{D}_1, u = v)$ algorithm, while delivering superior accuracy. The price to be paid is that we must calculate $\mathbf{D}_2\psi$ in addition to $\mathbf{D}_1\psi$ at each time step, but this is more than compensated by the high accuracy that can be achieved with a small number of grid points.

V. Extension to Three Dimensions

The previous developments can be extended to three dimensions. Here there are three different second-order FD Laplacians and two angular degrees of freedom.

In three dimensions (3a) and (3b) become

$$\begin{aligned} h^2\mathbf{D}_1 f(x,y,z) &= f(x+h,y,z)+f(x-h,y,z) \\ &\quad + f(x,y+h,z)+f(x,y-h,z) \\ &\quad + f(x,y,z+h)+f(x,y,z-h) \\ &\quad - 6f(x,y,z) \end{aligned} \tag{24a}$$

$$\begin{aligned} h^2\mathbf{D}_2 f(x,y,z) &= \frac{1}{4}[f(x+h,y+h,z+h)+f(x-h,y-h,z-h) \\ &\quad + f(x+h,y-h,z+h)+f(x-h,y+h,z-h) \\ &\quad + f(x-h,y+h,z+h)+f(x+h,y-h,z-h) \\ &\quad + f(x-h,y-h,z+h)+f(x+h,y+h,z-h)] \\ &\quad - 2f(x,y). \end{aligned} \tag{24b}$$

The third FD Laplacian can be constructed by combining two-dimensional Laplacians of the form (3b), for each of the three possible coordinate pairs

$$\mathbf{D}_3 = \frac{1}{2}\left(\mathbf{D}_2^{(xy)} + \mathbf{D}_2^{(xz)} + \mathbf{D}_2^{(yz)}\right). \tag{24c}$$

We obtain k-domain expressions analogous to (5) of the form

$$D_1(k,\theta,\phi) = \cos k_x + \cos k_y + \cos k_z - 3, \tag{25a}$$

$$D_2(k,\theta,\phi) = \cos k_x \cos k_y \cos k_z - 1 \tag{25b}$$

and

$$\begin{aligned} D_3(k,\theta,\phi) &= \frac{1}{2}(\cos k_x \cos k_y + \cos k_x \cos k_z \\ &\quad + \cos k_y \cos k_z - 3) \end{aligned} \tag{25c}$$

where $(k_x, k_y, k_z) = k(\sin\theta\cos\phi, \sin\theta\sin\phi, \cos\theta)$, and θ and ϕ are the usual spherical coordinates.

Fixing k, we now seek an isotropic linear combination of $\mathbf{D}_1$, $\mathbf{D}_2$, and $\mathbf{D}_3$, $\mathbf{D}_0 = \alpha_1\mathbf{D}_1 + \alpha_2\mathbf{D}_2 + \alpha_3\mathbf{D}_3$, such that $D_0 = \alpha_1 D_1 + \alpha_2 D_2 + \alpha_3 D_3 \approx \cos k - 1$ for all θ and ϕ. First we construct $\mathbf{D}_{12} = \gamma_{12}\mathbf{D}_1 + (1-\gamma_{12})\mathbf{D}_2$ and $\mathbf{D}_{13} = \gamma_{12}\mathbf{D}_1 + (1-\gamma_{13})\mathbf{D}_3$ and minimize the variation of $D_{12} = \gamma_{12}D_1 + (1-\gamma_{12})D_2$ and $D_{13} = \gamma_{13}D_1 + (1-\gamma_{13})D_3$ with respect to θ at $\phi = 0$. Following previous developments, we find $\gamma_{12} = \gamma_0$, and $\gamma_{13} = 2\gamma_0 - 1$, where γ_0 is given by (8). $\mathbf{D}_{12}$ and $\mathbf{D}_{13}$ are nearly isotropic with respect to θ, but not ϕ. Setting $\theta = \pi/4$ we suppress the ϕ-dependence of the combination

$$\mathbf{D}_0 = \eta_0\mathbf{D}_{12} + (1-\eta_0)\mathbf{D}_{13}. \tag{26}$$

Again following previous developments we find that the anisotropy of $D_0 = \eta_0 D_{12} + (1-\eta_0)D_{13}$ with respect to ϕ is minimized by choosing $\eta = \eta_0$, where

$$\eta_0(k) \equiv \frac{D_{13}(k,\pi/4,\phi_0) - (\cos k - 1)}{D_{13}(k,\pi/4,\phi_0) - D_{12}(k,\pi/4,\phi_0)} \tag{27}$$

where $\phi_0 \approx 0.11811\pi$. Since $D_0(k,\theta,0) = D_0(k,\theta)$, the θ-dependence of D_0 can be characterized by Fig. 1(b), while its ϕ-dependence, best characterized by $D_0(k,\pi/4,\phi)$, is shown in Fig. 4. As we can see in Figs. 1(b) and 4, the fractional variation of $D_0(k,\theta,\phi)$ about $\cos k - 1$ is approximately 10^{-6}, so (9) also holds in three dimensions.

$\mathbf{D}_0$ can now be expressed in the form

$$\mathbf{D}_0 = \alpha_1\mathbf{D}_1 + \alpha_2\mathbf{D}_2 + \alpha_3\mathbf{D}_3 \tag{28}$$

where

$$\begin{aligned} \alpha_1 &= \eta_0(1-\gamma_0) + (2\gamma_0 - 1) \\ \alpha_2 &= \eta_0(1-\gamma_0) \\ \alpha_3 &= 1 - (\alpha_1 + \alpha_2). \end{aligned} \tag{29}$$

Next let us examine stability. Extending the previous developments, to three dimensions we find

$$v_{\max}(\mathbf{D} = \mathbf{D}_1, u = v) = \frac{\sqrt{3}}{3} \approx 0.57. \tag{30}$$

For $(\mathbf{D} = \mathbf{D}_0, u = u_0)$ using $\lim_{k\to 0}\alpha_1(k) = 7/15$ and $\lim_{k\to 0}\alpha_2(k) = 2/15$, we find that $\max(-D) = 46/15$, which yields $u_0^2 < 15/23$. Repeating previous considerations we obtain

$$v_{\max}(\mathbf{D} = \mathbf{D}_0, u = u_0) = \frac{3}{\pi}\arcsin\left(\sqrt{\frac{15}{23}}\frac{\sqrt{3}}{2}\right) \approx 0.73. \tag{31}$$

In three dimensions $v_{\max}(\mathbf{D} = \mathbf{D}_0, u = u_0)$ is thus about 28% larger than $v_{\max}(\mathbf{D} = \mathbf{D}_1, u = v)$.

In three dimensions, using the $(\mathbf{D} = \mathbf{D}_0, u = u_0)$ algorithm, we achieve the same reduction (10^{-4}) in solution error as in two dimensions. Now however we must calculate $\mathbf{D}_2\psi$ and $\mathbf{D}_3\psi$ in addition to $\mathbf{D}_1\psi$ at each time step, but this is more than compensated by the high accuracy that can be achieved with a low number of grid points and by a reduction in the number of iterations needed.

VI. Boundary Conditions at the Subgrid Level

To apply the algorithm to solve practical problems on a coarse grid, it becomes important to implement boundary conditions at the subgrid level. For example for a TM wave in a complicated metal structure we would like to be able to implement the condition $E_z = 0$ at a metal boundaries without using a large number of grid points to describe their locations.

The boundary conditions of greatest interest are

$$\psi(x_B) = b \tag{32a}$$

$$\mathbf{n} \bullet \nabla\psi(x_B) = b \tag{32b}$$

where b is a constant, $\mathbf{n}$ is a local normal to the boundary, B, and $x_B \in B$. The basic problem is to approximate $\nabla^2\psi(x,t)$ in the neighborhood of a boundary point in terms of the boundary conditions and known field quantities inside the boundary while eliminating unknowns outside it, when x_B falls between the lattice points on the grid. To illustrate how (32a) and (32b) can be implemented in this case, consider a one-dimensional vibrating string. At $x_B = n + a$, where $0 < a < 1$, and n is an integer, (32a) becomes $\psi(n+a,t) = b$. Assuming that waves impinge on the boundary from the region $x < n + a$, we seek a FD expression for $\partial_{xx}\psi(n,t)$ in terms

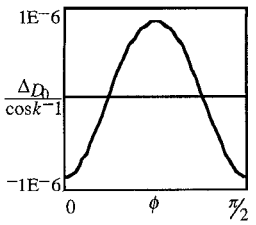

Fig. 3. Anisotropy of $\mathbf{D}_0$ in the azimuthal direction, where $\Delta D_0(k, \pi/4, \phi) = D_0(k, \pi/4, \phi) - (\cos k - 1)$ at $k = 2\pi/8$. Variability with respect to ϕ is maximal at $\theta = \pi/4$.

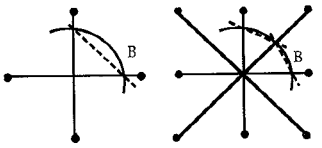

Fig. 4. $\psi(x_B)$ = constant on a curved boundary (B) that passes between the grid points. Dotted straight line segments indicate the effective approximation to B for the cases (a) $\mathbf{D} = \mathbf{D}_1$ and, (b) $\mathbf{D} = \mathbf{D}_0$.

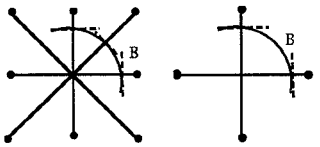

Fig. 5. $\mathbf{n} \bullet \nabla\psi(x_B)$ = constant on a curved boundary (B) that passes between the grid points, where $\mathbf{n}$ is a local normal. Dotted straight line segments indicate the effective approximation to B for the cases (a) $\mathbf{D} = \mathbf{D}_1$ and, (b) $\mathbf{D} = \mathbf{D}_0$.

of $\psi(n+a,t)$, $\psi(n,t)$, and $\psi(n-1,t)$. Expanding $\psi(n+a,t)$ and $\psi(n-1,t)$ in Taylor series about $x = n$, we obtain

$$\partial_{xx}\psi(n,t) \approx \frac{2}{a(1+a)}[a\psi(n-1,t) - (1+a)\psi(n,t) + b]. \tag{33a}$$

This result can be generalized to higher dimensions. The extension of (33a) to two dimensions using $\mathbf{D} = \mathbf{D}_1$ is equivalent to approximating B by the dashed line as shown in Fig. 4(a), while using $\mathbf{D} = \mathbf{D}_0$ is equivalent to the approximation shown in Fig. 4(b).

Returning to the string, (32b) takes the form $\partial_\tau\psi(n+a,t) = b$, and it is easy to show that

$$\partial_{xx}\psi(n,t) \approx \frac{1}{a+1/2}[\psi(n-1,t) - \psi(n,t) + b]. \tag{33b}$$

This result can also be extended to higher dimensions. In two dimensions, using $\mathbf{D} = \mathbf{D}_1$, (33b) is equivalent to approximating B by tangents perpendicular to the coordinate axes as shown in Fig. 5(a), while using $\mathbf{D} = \mathbf{D}_0$ is equivalent to approximating B as shown in Fig. 5(b).

VII. Summary

In this paper we have derived a new FD approximation to the wave equation for use on a coarse grid to solve wave propagation and scattering problems in complicated environments. Using just eight grid units per wavelength ($\lambda/h = 8$) the solution error is less than 10^{-4} that of the conventional FDTD algorithm using $(\mathbf{D} = \mathbf{D}_1, u = v)$. To attain the same accuracy with the $(\mathbf{D} = \mathbf{D}_1, u = v)$ algorithm one would need to operate at $\lambda/h = 1140$.

This superior accuracy comes at the expense of a greater computational load at each grid point, but it is more than offset by the low λ/h ratio that can be used, as well as by a decrease in the number of iterations needed. In addition, boundaries can be more accurately characterized. Although optimal performance can be achieved at only one frequency, good results can still be had with multifrequency signals.

Our algorithm is based on an isotropic second-order FD Laplacian, which can be used in FD approximations to other differential equations. The same approach used to construct it can be applied to derive other kinds of isotropic FD operators.

Appendix A
Application to Multifrequency Signals

Since both $\mathbf{D}_0$ and u_0 are functions of k, the $(\mathbf{D} = \mathbf{D}_0, u = u_0)$ solution error rises for spatial frequencies that deviate from the value, k_0, at which $\mathbf{D}_0$ and u_0 are defined. The smaller k_0, the smaller the solution error away from k_0. Even on a coarse grid ($\lambda \sim 8$), however, the maximum anisotropy of $\mathbf{D}_0(k_0)e^{\imath k\bullet x}/e^{\imath k\bullet x}$ is still less than 10^{-2} that of $\mathbf{D}_1 e^{\imath k\bullet x}/e^{\imath k\bullet x}$, so $\mathbf{D}_0(k_0)e^{\imath k\bullet x}/e^{\imath k\bullet x} \approx 2(\cos k - 1)$ is still a reasonable approximation even at $k \neq k_0$. The main source of solution error at $k \neq k_0$ thus arises from the difference between $\mathbf{D}_0(k_0)e^{\imath k\bullet x}/e^{\imath k\bullet x} \approx 2(\cos k - 1)$ and $\mathbf{D}_0(k_0)e^{\imath k_0\bullet x}/e^{\imath k_0\bullet x} \approx 2(\cos k_0 - 1)$. To handle broadband signals one should therefore set the (smallest) wavelength, λ_L (in terms of grid units), corresponding to the highest wavenumber, k_H, such that the difference, $(\cos k_L - \cos k_H)$, is "sufficiently" small, where k_L is the lowest wavenumber. The broader the frequency range, the larger λ_L must be for a given error tolerance, and hence the finer the grid relative to the wavelengths. "Sufficiently small" depends on the details of the particular problem at hand, such as signal bandwidth, the maximum propagation distance and the tolerable phase error.

Appendix B
Space-Time Sampling of the Wavefield

Let f be a function of the form $f(x) = a\sin kx + b\cos kx$ on a one-dimensional grid, where $k = 2\pi/\lambda$. For $\lambda = 1$ and 2 (grid units) the sine component of the signal vanishes at the sample points. To unambiguously determine both a and b on a discrete interval of length λ, at least four sample values are needed. We thus obtain the constraint $\lambda \geq 3$. For the $(\mathbf{D} = \mathbf{D}_1, u = v)$ case this constraint applies in both two and three dimensions, for $(\mathbf{D} = \mathbf{D}_0, u = u_0)$, however, the calculation of $\mathbf{D}_0\psi$ involves grid points that are separated by a distance of $\sqrt{d}$, where d is the dimensionality of the grid, thus for $\mathbf{D} = \mathbf{D}_0$ we must satisfy

$$\lambda \geq 3\sqrt{d}. \tag{B1}$$

Rounding off to next highest integer values gives $\lambda \geq 5$, and $\lambda \geq 6$ in two, and three dimensions, respectively. We have

used $\lambda = 8$ in our calculations in order to resolve the peaks and troughs of the wavefields.

ACKNOWLEDGMENT

The author would like to thank R. A. Krutar (NRL) for helpful suggestions and comments. A. R. Haralampus, a teacher at Bishop O'Donnel High School, and E. Kirkland, a student at Gwynn Park High School, who spent the summer of 1993 here under SEAP Program, casting these equations into a working computer code, and verifying that the new algorithm actually worked. Without their efforts this paper could not have been written.

REFERENCES

[1] S. K. Godunov, *Difference Schemes*. Amsterdam: North-Holland, 1987.
[2] J. M. Pearson, *A Theory of Waves*. Boston: Allyn and Bacon, 1966.
[3] J. B. Cole, R. A. Krutar, S. K. Numrich, and D. B. Creamer, "A cellular automaton methodology for solving the wave equation," in *Proc. 7-th ACM/SIGARCH Int. Conf. Supercomputing*, Tokyo, 1993.
[4] R. A. Krutar *et al.*, "Computation of acoustic field behavior using a lattice gas model," in *Proc. Oceans 91 Conference*, vol. 1, Honolulu, 1991, pp. 446–452.
[5] S. K. Numrich, R. A. Krutar, and R. Squier, "Computation of acoustic fields on a massively parallel processor using lattice gas methods," in *Computational Acoustics, Proc. 3rd IMACS (Int. Asso. for Mathematics and Computers in Simulation) Symp.*, R. D. Lau *et al.*, Eds., 1991.
[6] R. E. Mickens, "A new finite-difference scheme for schroedinger type partial differential equations," in *Computational Acoustics*, D. Lee, A. R. Robinson, and R. Vichnevetsky, eds., vol. 2. Amsterdam: Elsevier, 1993, pp. 233–239.
[7] O. Maeshima, T. Uno, Y. He, and S. Adachi, "FDTD analysis of two-dimensional cavity-backed antenna for subsurface radar," *IECE Trans. Electron.*, vol. E-76-C, no. 10, pp. 1468–1473, Oct. 1993.

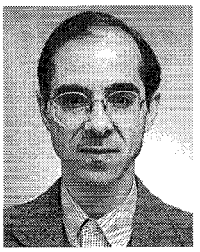

James B. Cole received the B.S. degree in physics from the Illinois Institute of Technology in 1972, the M.S. degree in information engineering from the University of Illinois-Chicago in 1981, and the Ph.D. degree in physics from the University of Maryland in 1987.

He became interested in his present field, interdisciplinary problems on the boundary between electrical engineering, information science and physics, as a result of his postdoctoral experience at the NASA Goddard Space Flight Center where he worked on modeling a possible production mechanism for antiprotons in the earth's atmosphere, and while working on new types of high energy particle detectors. He joined the Army Research Laboratory in 1988. He was an invited Guest Scientist in Japan at Nippon Telephone and Telegraph Corporation's Basic Research Laboratory in 1990, where he applied group theory and differential geometry to human and computer vision problems. He was also at the Physical-Chemical Research Institute in 1994, where worked on electromagnetic problems. He has been with the Naval Research Laboratory in Washington, DC since 1990 where he has been working on parallel algorithms to simulate wave propagation and scattering in complicated environments coupled with advanced visualizations.